Conference Paper

Numerical optimisation of air-cooled heat sink geometry to improve temperature gradient of power semiconductor modules

Sharp, A., Niedermayer, J.M., Akinsolu, M.O., Vagapov. Y., Monir, S., and Dianov, A.

This is a paper presented at XV Int. Symp. on Industrial Electronics and Applications INDEL-2024, Banja Luka, Bosnia and Herzegovina, 6-8 Nov. 2024.

The published version is available at: https://ieeexplore.ieee.org/document/10772679

Numerical Optimisation of Air-cooled Heat Sink Geometry to Improve Temperature Gradient of Power Semiconductor Modules

Andrew Sharp
Wrexham University
Wrexham, UK

Julian M. Niedermayer
Wrexham University
Wrexham, UK

Mobayode O. Akinsolu
Wrexham University
Wrexham, UK

Yuriy Vagapov
Wrexham University
Wrexham, UK

Shafiul Monir
Wrexham University
Wrexham, UK

Anton Dianov
Pingyang Institute of Intelligent Manufacturing
Wenzhou University
Wenzhou, China

***Abstract*—This paper discusses the numerical analysis and optimisation of a conventional air-cooled heat sink having an insignificant geometrical modification to reduce the temperature gradient of power semiconductors installed on the top surface of the heat sink. Using the numerical approach, the influence of the geometry modification on the thermal performance of the heat sink was thoroughly analysed. The geometry modification applied to the heat sink is based on the partial removal of the central fins at the air flow intake in the form of a triangle and the integration of a guide plate to provide a reduction in the temperature difference across the heat sink surface. These modifications do not expand the heat sink footprint or make the manufacturing process complicated. The optimised design exhibited a considerably reduced temperature gradient between the power electronic modules. The temperature difference between power semiconductors operating with a power loss of 100 W per module is reduced from 3.779°C (for the unmodified benchmark model) to 0.0018°C. The study findings contribute to the advancement of thermal solutions in power electronics by presenting a manufacturable, scalable, and efficient heat sink design that addresses the industry demand for sustainable thermal regulation.**

Keywords—heat sink, temperature gradient, power electronic module, IGBT, power semiconductor reliability, CFD

I. Introduction

The demand for high-performance power electronics has dramatically increased in the last decades for a wide variety of industrial and domestic applications including transportation, electrical power processing/delivery, energy storage installations, etc. Design and implementation of robust power electronic systems have become a prerequisite for ensuring the reliability and prolonged operational lifespan of electrical systems [1],[2]. As reported in [3], power electronics components contribute 31% of the failures occurring in power converters, of which 55% are related to power semiconductor overheating. Therefore, significant attention is paid to solving problems related to the thermal management of power electronic devices which are affected by mechanical stress due to temperature variations and temperature gradients during operation in high-power systems. Mechanical stress can potentially lead to fatigue of the semiconductor structure and metal bonds resulting in performance degradation, lifetime reduction, and failure [4], [5]. This problem highlights the importance of studying the temperature distribution within heat sinks used as conventional cooling devices for power semiconductors [6]-[8].

In the realm of power electronics, efficient thermal management is pivotal to the reliability and performance of power semiconductor devices such as insulated-gate bipolar transistors (IGBT). This study introduces a novel approach to the design of a heat sink aimed at optimising the thermal gradient between IGBT modules. Involving computational fluid dynamics and thermal simulations using Ansys Workbench R2 2023, a model was developed that simulates the complex heat transfer mechanisms inherent in power electronic systems.

Initially, a benchmark model was developed to replicate the exact geometric dimensions and environmental conditions typical of a standard heat sink configuration. This model was built in Autodesk Inventor 2024, where the setup included the precise layout of the heat sink fins and the positioning of the IGBT modules. Precious determination of the mesh sizing is critical to the success of the Computational Fluid Dynamics (CFD) simulation. Mesh sizing for this study was optimised through multiple trials to ensure a balance between computational efficiency and the accuracy of the results. The simulation parameters were thoroughly defined in the Fluent Setup to accurately reflect real-world conditions. These parameters include the energy model, the viscous model, the material properties of the heat sink, and the airflow dynamics, with a particular focus on approximating the effects of passive convection.

Following the establishment of a robust benchmark, the study proceeded to explore modifications to the heat sink geometry, specifically targeting the optimisation of the fin arrangement considering the airflow and cooling efficiency. This phase involved employing a Design of Experiments (DOE) and response surface methodology to systematically evaluate the impact of various geometrical changes. Through these methods, the study identified specific modifications that could potentially minimise the temperature difference across the heat sink surface.

The optimisation process identified that modifying certain fins can significantly influence the airflow pattern and cooling efficiency. These findings lead to a set of geometric adjustments that promise to improve thermal management without requiring an increase in the system footprint or manufacturing complexity.

By utilising advanced simulation tools, the project replicated the conditions of a physical test rig and predicted the thermal behaviour under modified conditions, thus guiding further enhancements. This approach ensures that the heat sink design is effective in reducing temperature gradients and is viable in terms of manufacturing and

979-8-3503-5232-0/24/$31.00 ©2024 IEEE

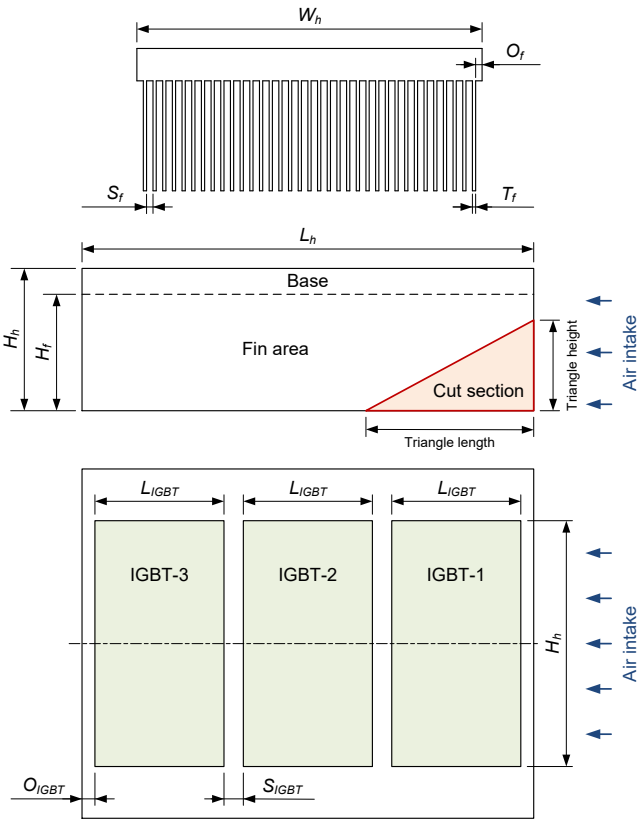

Fig. 1. Geometry of the heat sink.

operational efficiency, marking a significant step forward in thermal management solutions for power electronics.

A previous study has identified that there are two important factors to consider in such an approach: (1) the maximum temperature of semiconductor devices, (2) the temperature distribution/temperature gradient across the heat sink length [9]. The effect of the temperature gradient is considered to be more detrimental to the component life, due to the generation of mechanical stresses, than the maximum temperature, providing the maximum temperature does not exceed the maximum rated junction temperature of the device [9].

The heat sink selected for this study is the same used for practical tests in the test rig for thermal investigations. Upon completion of the model simulation, the practical experiment is planned in the test rig. The test rig where parameters such as heat sink temperature and air flow mass can be measured [10]. The test rig was set up to include an air-cooled heat sink on which three IGBT modules were mounted, and a CFD model was created to simulate the parameters of this arrangement.

TABLE I. DIMENSIONS OF THE HEAT SINK.

Symbol	Type	Value
L_h	Heat sink length	210 mm
L_{IGBT}	IGBT-Module length	58 mm
H_h	Heat sink height	67 mm
H_f	Fin height	56.2 mm
W_h	Heat sink width	167 mm
W_{IGBT}	IGBT-Module width	122 mm
T_f	Fin thickness	1 mm
S_f	Fin spacing	3.5 mm
S_{IGBT}	IGBT-Module spacing	10 mm
O_f	Fin offset	2 mm
O_{IGBT}	IGBT-Module offset	8 mm

II. BENCHMARK HEAT SINK MODEL

The geometry of the heat sink was modelled in Autodesk Inventor 2024 and then imported into Ansys Design Modeler and modified further. Three-dimensional models were generated using the Ansys Design Modeler and transferred to Ansys Meshing. Using Ansys Meshing, it was then prepared for Ansys Fluent.

Due to its reliability and proven accuracy, the standard k − ε model was selected. The standard k − ε model is a well-established two-equation turbulence model widely recognised for its robustness, computational efficiency, and satisfactory accuracy across a broad spectrum of turbulent flows. This has made the model very popular in practical engineering flow calculations, especially in the industrial field of flow and heat transfer simulations [11]-[13]. The k − ε model offers the dual benefit of determining both turbulent length and time scales by solving two distinct transport equations. Its semiempirical nature stems from a combination of empirical evidence and phenomenological underpinnings. The model equations derived from these grounds have demonstrated reliable performance in various applications, contributing to its widespread adoption in computational fluid dynamics [11].

The reference benchmark model must be as close to reality as possible, so it was based on a real physical artefact from which the measurements were taken, and it was these parameters that formed the basis of the benchmark model.

A. Geometry

Measurements were taken from the physical heat sink to construct a three-dimensional model, derived from a CAD drawing constructed using Autodesk Inventor 2024. Although three IGBT modules were mounted on the physical heat sink, for ease of viewing, only the contours of their contact surfaces are shown in the drawing (Fig. 1). The dimensions of the heat sink are shown in Table I.

B. Heat Sink Material

The physical heat sink is made of aluminium, although the precise composition is not known. This represents an uncertain factor in this study, since the thermal conductivity of aluminium varies with its chemical composition [14]. An aluminium alloy with a thermal conductivity coefficient of 201 W/m·K is a material commonly used in industry [15]. Therefore, this value was also selected for the benchmark model.

C. IGBT Modules

The system consists of three IGBT modules mounted on the physical heat sink. A power loss in the range from 50 W to 100 W per IGBT module was used for the CFD modelling, as it corresponds to the power losses achievable using the test rig [9]. These parameters also fall well within the maximum power loss of the IGBT modules provided by the semiconductor manufacturer [16]. The modules used for this study are Toshiba Silicon N-Channel IGBT MG400Q2YS60A.

The IGBT temperature is defined as the area-weighted average of the total temperature of the contact surface with the heat sink. The indirect criterion for the temperature

gradient analysis is derived as the temperature difference between the average temperature of the third (hottest) IGBT module T_{IGBT3} and the average temperature of the first (coolest) IGBT module T_{IGBT1}. Following this approach, the temperature difference (ΔT) is defined as

$$\Delta T = T_{IGBT3} - T_{IGBT1} \quad (1)$$

As IGBTs can be operated in the test rig with a maximum power loss of 100 W per module [9], this represents the most extreme scenario considered for the benchmark model. The contact surface area of the IGBT modules must be considered to determine the heat flux into the heat sink. This results in a heat flux of 14132 W/m^2 per module.

D. Airflow

The fan produces airflow at the intake cross-section, which has been measured at approximately 5 m/s. The ambient temperature of the test rig varies with the season and time of day. A typical measured value is 20°C. Both values are selected for simulation: 5 m/s for the airflow speed and the ambient temperature of 20°C for the air intake.

E. Passive Convection

In reality, the heat sink is surrounded by still air, which assists in cooling it by transferring heat from the heat sink to the air molecules. This phenomenon is not simulated to maintain performance requirements and complexity within reasonable limits. Instead, the effect is accounted for through the convective heat transfer coefficient h [W/m^2·K]. To determine an appropriate value, simulations have been performed to observe its effect on the temperature gradient.

As Fig. 2 illustrates, the impact of the convective heat transfer coefficient h on the temperature delta is relatively modest. However, the temperature gradient is observed to decrease with increasing h. To prevent the benchmark results from being artificially inflated, a conservative value should be selected. A value of 5 W/m^2 K has been selected as an appropriate choice. This is also corroborated by the basic calculations in [17].

F. Benchmark Model Parameters

Table II illustrates the relevant parameters employed in the benchmark model. To prevent the results of the research from being artificially inflated, these parameters are used in both the benchmark model and the geometrically modified model.

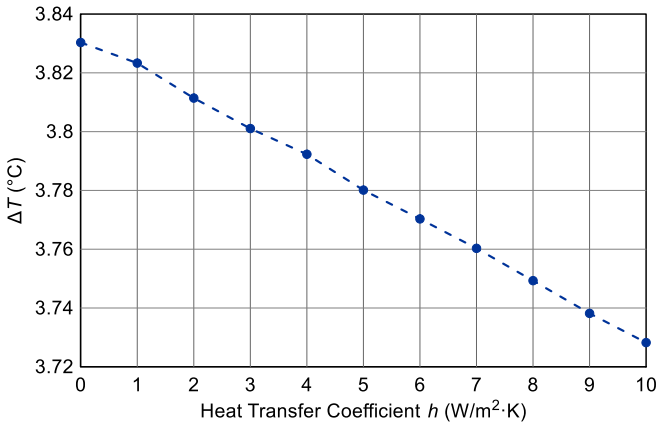

Fig. 2. Convective heat transfer coefficient vs ΔT.

TABLE II. SUMMARY OF PARAMETERS FOR BENCHMARK MODEL.

Parameter	**Value**
Mesh element size	1.5 mm
Turbulence Model	standard k − ε
Enhanced Wall Treatment	active
Thermal effects	active
Heat sink material	aluminium
Thermal conductivity coefficient	201 W/m·K
Air temperature	20°C
Air intake speed	5 m/s
Convective heat transfer coefficient	5 W/m^2·K
IGBT power loss per module	100 W
IGBT heat-flux per module	14132 W/m^2

G. Benchmark Model Parameters

Modelling using the benchmark model demonstrates the temperature gradient on the top surface of the heat sink from the air intake to the outlet. This directly translates into temperature differences in the IGBT modules mounted on the heat sink. The temperatures calculated as the area-weighted average of the total temperature of the contact surface for the respective IGBT module are as follows: the temperature of IGBT-1 is 33.10°C, the temperature of IGBT-2 is 35.31°C, and the temperature of IGBT-3 is 36.88°C. Therefore, the temperature difference introduced as an indirect gradient criterion according to (1) is ΔT = 3.78°C.

III. MODIFIED MODEL OF HEAT SINK

In order to reduce the temperature gradient across the heat sink, it is necessary to modify its geometry. The objective is to keep the modification as simple as possible to keep the modification costs low and to avoid increasing either the footprint of the original heat sink or increasing the space required for airflow; this approach maintains the requisite degrees of freedom for proper installation at a level comparable to that of the unmodified heat sink. Previous work has proposed a V-cut in the guide plate of the heat sink [6] and this modification is relatively straightforward and inexpensive, but it does require a greater volume of free space around the heat sink to ensure proper airflow. This happens because an additional air-inlet surface is created.

A. Geometry

The modification for this study involves the partial removal of the middle fins of the heat sink. Physical modification could be performed on conventional three-axis

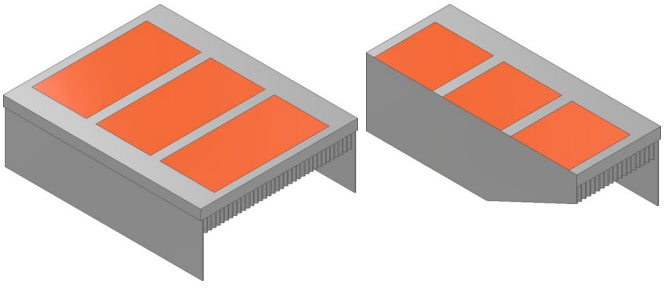

Fig. 3. Modified heat sink model.

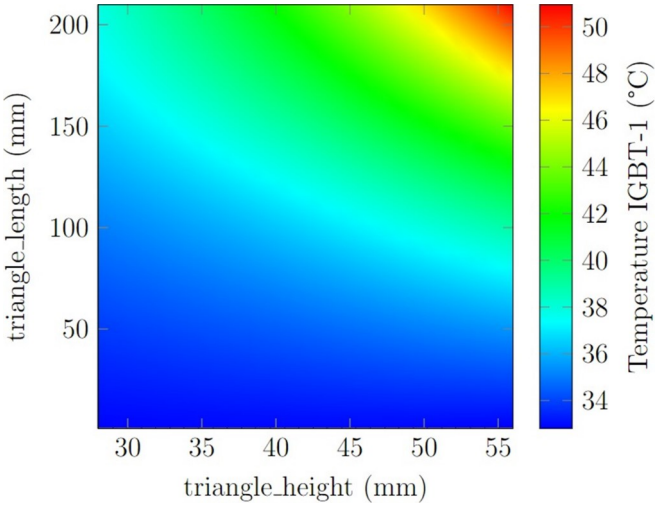

Fig. 4. Temperature IGBT-1.

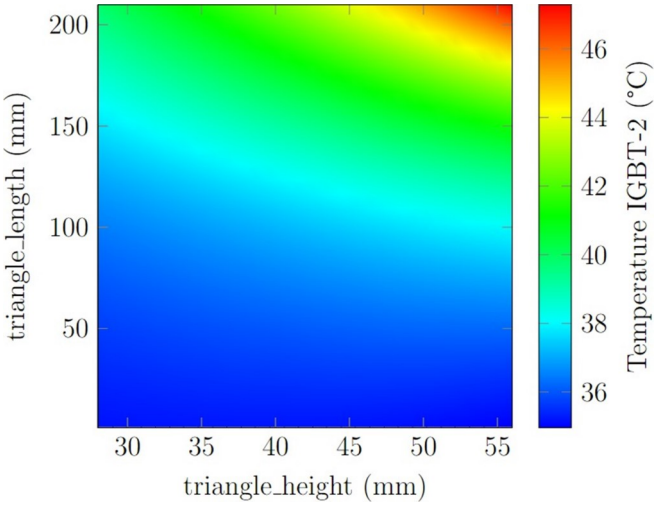

Fig. 5. Temperature IGBT-2.

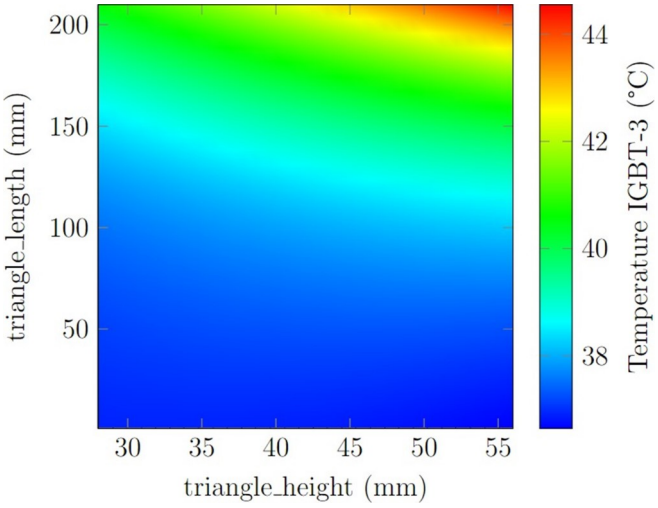

Fig. 6. Temperature IGBT-3.

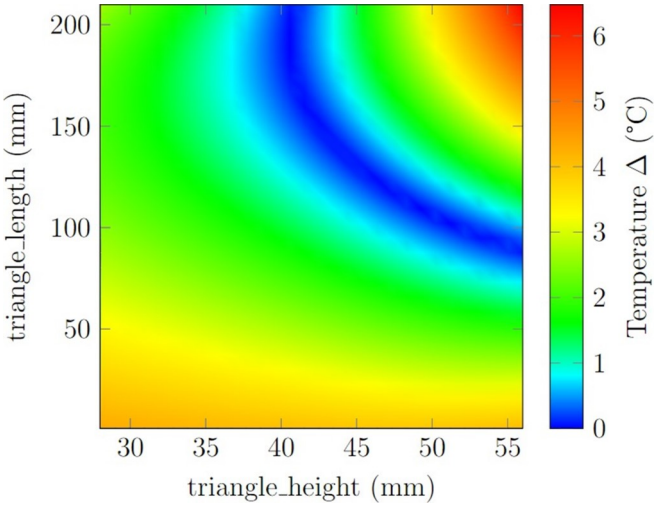

Fig. 7. Temperature ΔT.

milling machines [18]. Following this, a guide plate must be attached to the bottom of the heat sink. A triangle-cut section of the heat sink is removed as shown in Fig. 1.

From the 37 heat sink fins, the middle 35 are modified on the air intake side (Fig. 1). The removed material is outlined in red. The parameters "triangle height" and "triangle length" define the size and ratio of the triangle. Parametric modelling enables the creation of numerous versions of the modified model. The boundaries of the parameters are defined in Table III. Any combination of these two parameters within their boundaries will result in a model similar to the one shown in Fig. 3. Note that the two outer fins are fully intact to serve as a guide for the airflow.

TABLE III. TRIANGLE CUT SECTION BOUNDARIES.

Parameter	Value	Note
minimal triangle height	28 mm	Material removal would be minimal and the resulting effect on cooling performance would be negligible.
maximal triangle height	56 mm	Material removal would extend into the top base plate and damage the integrity of the heat sink.
minimal triangle length	1 mm	Triangle would not be properly defined
maximal triangle length	209.9 mm	Triangle would extend beyond base model and cause trouble with cut selection.

B. Optimisation

Fig. 4, Fig. 5, and Fig. 6 visualise how the temperature of the three IGBT modules is changed against the two input parameters under a load of 100 W per module. Heatmaps are chosen here for their capability to display a three-dimensional graph on a two-dimensional surface. Note that the scales for each heatmap are different, as indicated by the corresponding legend on the right-hand side of each figure. It can be observed that the IGBT temperatures reach their maximum where the input parameters are at their maximum. This is logical, as high values of triangle height and triangle length indicate a significant amount of material being removed. Consequently, the surface area of the heat sink is reduced, which in turn negatively affects the cooling performance; however, the increase in the overall temperature, particularly of IGBT-1 and IGBT-2 falls well within the maximum allowed junction temperature of the device [16].

Fig. 7 visualises the relation between the input parameters and the ΔT under a load of 100 W per module.

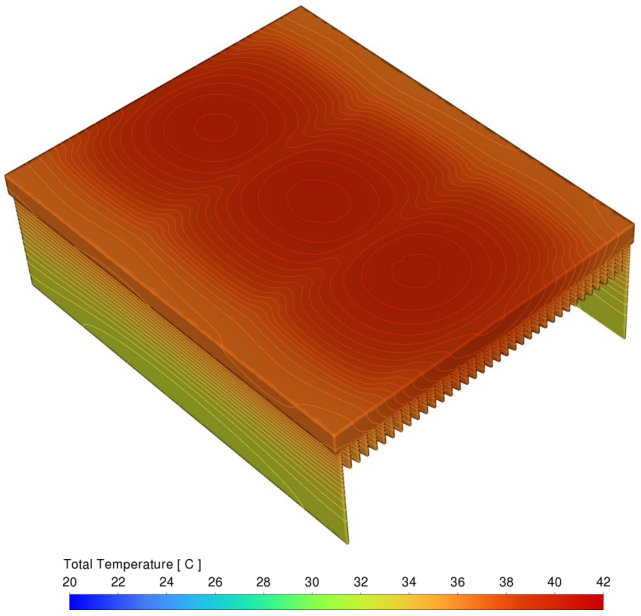

Fig. 8. Temperature gradient of the optimised model.

The values of ΔT are presented in terms of their absolute value, to highlight the dark blue area where ΔT passes through 0°C and thus reverses the temperature gradient. The change in colour shows the increase in ΔT from 0°C in both directions on the graph surface. Where ΔT approaches zero, enough material has been removed to increase the temperature of the IGBT-1, ensuring that it does not exceed the temperature of IGBT-3. The following information can be extracted from Fig. 7.

- It is possible for ΔT to reach 0°C.
- Excessive modification reverses the temperature gradient, indicated by the negative values of ΔT.
- There are a large number of combinations of the two parameters where ΔT is 0°C.
- A triangle height below 40 mm does not allow for ΔT to reach 0°C.
- A triangle length below 80 mm does not allow for ΔT to reach 0°C.

At any point where the response surface intersects the plane $\Delta T = 0$, a valid combination of "triangle height" and "triangle length" exists. This fact is used to identify possible combinations of parameters that result in $\Delta T = 0$.

Three candidate points were selected and their predicted ΔT value was verified through simulation, as illustrated in Table IV. The simulated ΔT values for all three candidates were found to be very close to 0°C. However, candidate Gamma exhibited the most promising results and was therefore subjected to further investigation. Its ΔT value was three orders of magnitude lower than that of the unmodified version. The temperature contour of the candidate Gamma can be observed in Fig. 8. The sole modification made to the model is the geometric alteration of the heat sink, defined by a triangle height of 42.525 mm and a triangle length of 144.772 mm. This optimal model is subject to further investigation, where the power loss per module varies.

TABLE IV. OPTIMUM CANDIDATE POINTS.

Candidate Point	Triangle height	Triangle length	Actual ΔT
Alpha	53.291 mm	93.091 mm	0.0369°C
Beta	40.750 mm	198.607 mm	0.0109°C
Gamma	42.525 mm	144.772 mm	−0.0018°C

TABLE V. COMPARISON OF BENCHMARK MODEL WITH OPTIMISED MODEL.

Power Loss per IGBT Module	Temperature ΔT	
	Benchmark Model	Optimised Geometry Model
50 W	1.892°C	0.006°C
60 W	2.267°C	0.009°C
70 W	2.647°C	0.009°C
80 W	3.024°C	0.012°C
90 W	3.403°C	0.014°C
100 W	3.779°C	−0.0018°C

IV. RESULTS

In further investigation of the optimised geometry shown in Table IV, it was found that the improved ΔT translates into lower loads without any changes in the geometrical model. It demonstrates that there is no need to implement optimisation for the remaining IGBT loads. This represents considerable savings in time and resources.

Table. V shows the comparison of the benchmark heat sink model and the optimised geometry model (Gamma candidate) in terms of the temperature difference ΔT for the load ranging from 50 W to 100 W. It can be seen that the optimised model performs consistently under any load.

V. CONCLUSION

This study employed a rigorous analytical approach to enhance the thermal management of heat sinks, which is vital for ensuring the reliability and lifetime of power electronics, such as IGBTs. By adopting a simulation-based approach, the research bypassed physical prototypes in favour of a cost-effective and swift optimisation process using Ansys Workbench R2 2023. The thorough replication of the geometric dimensions, environmental conditions, and operational parameters of the physical heat sink provided the foundation for a comprehensive benchmark model. Through this model, the study explored the intricacies of airflow dynamics and material properties for subsequent heat sink modifications aimed at reducing thermal gradients.

The investigation process yielded a modified heat sink design, characterised by the removal of material from the central fins and the incorporation of a tailored guide plate. This design, derived from the response surface methodology, showed an impressive reduction in the temperature gradient, performed consistently on a range of IGBT power losses without requiring further geometrical alterations, and did not expand the spatial requirements of the heat sink or overcomplicate its manufacturing process. The study shows that the temperature difference between IGBT modules having power loss of 100 W per module is significantly reduced from 3.779°C for the benchmark model to 0.0018°C for the optimised design. The study achieved its primary objective by identifying and validating a geometric modification that significantly diminished the temperature differential across the heat sink. This modification preserves the original heat sink footprint and ensures easy manufacturability, thereby presenting a practical and efficient solution for enhancing the thermal management of power electronic systems.

References

[1] S. Yang, A. Bryant, P. Mawby, D. Xiang, L. Ran, and P. Tavner, "An industry-based survey of reliability in power electronic converters," *IEEE Transaction on Industry Applications*, vol. 47, no. 3, pp. 1441–1451, 2011, doi: 10.1109/TIA.2011.2124436

[2] A. Dianov, "Inverter temperature monitoring of cordless tool motor drives," *IEEE Open Journal of the Industrial Electronics Society*, vol. 4, pp. 52–62, Jan. 2023, doi: 10.1109/OJIES.2023.3235357

[3] B. Gao, F. Yang, M. Chen, M. Dong, P. Duan, and U. Irfan, "A temperature spectrum density distribution based condition evaluation method and application in IGBT," *Applied Thermal Engineering*, vol. 106, pp. 1440–1457, 2016, doi: 10.1016/j.applthermaleng.2016.06.054

[4] J. Falck, C. Felgemacher, A. Rojko, M. Liserre, and P. Zacharias, "Reliability of power electronic systems," *IEEE Industrial Electronics* Magazine, vol. 12, no. 2, pp. 24–35, 2018, doi: 10.1109/MIE.2018.2825481

[5] Z. Khattak and H. M. Ali, "Air cooled heat sink geometries subjected to forced flow: A critical review," International *Journal of Heat and Mass Transfer*, vol. 130, pp. 141–161, 2019, doi: 10.1016/j.ijheatmasstransfer.2018.08.048

[6] C. Bünnagel, S. Monir, A. Sharp, A. Anuchin, O. Durieux, I. Uria, and Y. Vagapov, "Forced air cooled heat sink with uniformly distributed temperature of power electronic modules," *Applied Thermal Engineering*, vol. 199, 2021, Art no. 117560, doi: 10.1016/j.applthermaleng.2021.117560

[7] D. A. Murdock, J. E. Ramos Torres, J. J. Connors, and R. D. Lorenz, "Active thermal control of power electronic modules," *IEEE Transaction on Industry Applications*, vol. 42, no. 2, pp. 552–558, 2006, doi: 10.1109/TIA.2005.863905

[8] A. Anuchin, V. Podzorova, V. Popova, I. Gulyaev, F. Briz, and Y. Vagapov, "Model predictive torque control of a switched reluctance drive with heat dissipation balancing in a power converter," in *Proc. IEEE 60th Int. Sci. Conf. on Power and Electrical Engineering of Riga Technical University*, Riga, Latvia, 2019, pp. 1–6, doi: 10.1109/RTUCON48111.2019.8982255

[9] A. Sharp, S. Monir, Y. Vagapov, and R. J. Day, "Temperature gradient improvement of power semiconductor modules cooled using forced air heat sink," in *Proc. XIV Int. Symp. on Industrial Electronics and Applications*, Banja Luka, Bosnia and Herzegovina, 2022, pp. 1–5, doi: 10.1109/INDEL55690.2022.9965507

[10] A. Sharp, S. Monir, R. J. Day, Y. Vagapov, and A. Dianov, "A test rig for thermal analysis of heat sinks for power electronic applications," in *Proc. IEEE East-West Design and Test Symposium*, Batumi, Georgia, 2023, pp. 1–4, doi: 10.1109/EWDTS59469.2023.10297055

[11] ANSYS, "Ansys fluent theory guide", 2021. Accessed: Jun. 12, 2024. [Online]. Available: www.cfdexperts.net

[12] A. Zhang and Y. Li, "Thermal conductivity of aluminum alloys—A review," *Materials*, vol. 16, no. 8, 2023, Art no. 2972, doi: 10.3390/ma16082972

[13] A. Mueller, C. Buennagel, S. Monir, A. Sharp, Y. Vagapov, and A. Anuchin, "Numerical design and optimisation of a novel heatsink using ANSYS steady-state thermal analysis," in *Proc. 27th Int. Workshop on Electric Drives (IWED)*, Moscow, Russia, 2020, pp. 1–5, doi: 10.1109/IWED48848.2020.9069568

[14] A. Anuchin, F. Briz, I. Gulyaev, A. Zharkov, M. Gulyaeva, and V. Popova, "Heat dissipation balancing in a switched reluctance drive by combined use of active and passive thermal control methods," in *Proc. 20th Int. Symp. on Power Electronics*, Novi Sad, Serbia, 2019, pp. 1–5, doi: 10.1109/PEE.2019.8923285

[15] M. Ekpu, R. Bhatti, N. Ekere, and S. Mallik, "Advanced thermal management materials for heat sinks used in microelectronics," in *Proc. 18th European Microelectronics and Packaging Conference*, Brighton, UK, 2011, pp. 1–8.

[16] Toshiba, "MG400Q2YS60A". Accessed: Jun. 12, 2024. [Online]. Available: http://www.ceipsa.com/datasheet/MG400Q2YS60A.pdf

[17] H. B. Awbi, "Calculation of convective heat transfer coefficients of room surfaces for natural convection," *Energy and Buildings*, vol. 28, no. 2, pp. 219–227, 1998, doi: 10.1016/S0378-7788(98)00022-X

[18] Z. Abd Rahman, S. B. Mohamed, A. R. Zulkifli, M. S. Kasim, and W. N. F. Mohamad, "Design and fabrication of a PC-based 3 axis CNC milling machine," *International Journal of Engineering Trends and Technology*, vol. 69, no. 9, pp. 1–13, 2021, doi: 10.14445/22315381/IJETT-V69I9P201